Human Pathology (2019) **84**, 62–70

ELSEVIER

Human PATHOLOGY

www.elsevier.com/locate/humpath

Original contribution

High expression of SLC17A9 correlates with poor prognosis in colorectal cancer☆,☆☆

Liang Yang MD[a,1], Zhihui Chen MD[a,1], Weixin Xiong MD[a], Hui Ren MD[a], Ertao Zhai MD[a], Kaiwu Xu MD[a], Hong Yang MD[a], Zhimei Zhang MD[b], Li Ding MD[b], Yulong He MD[a], Xinming Song MD[a,*], Jia Liu MD[c,]**

[a]*Department of Gastrointestinal Surgery, First Affiliated Hospital, Sun Yat-sen University, Guangzhou 510080, China*
[b]*Department of Pathology, First Affiliated Hospital, Sun Yat-sen University, Guangzhou 510080, China*
[c]*Department of Respiratory Medicine, Guangdong Second People's Hospital, Guangzhou 510317, China*

Received 18 June 2018; revised 6 September 2018; accepted 10 September 2018

Keywords:
SLC17A9;
Colorectal cancer;
Prognosis

Summary Solute carrier family 17 member 9 (SLC17A9) is a member of the family of transmembrane proteins that are involved in the transport of small molecules. The role of SLC17A9 in colorectal cancer (CRC) remains poorly understood. The present study aimed to demonstrate the clinicopathological significance and prognostic role of SLC17A9 in CRC. Here, we firstly analyzed the data from The Cancer Genome Atlas on SLC17A9 expression in CRC data sets and detected SLC17A9 expression level in 8 pairs of fresh CRC tissues and adjacent nontumorous tissues by quantitative real-time reverse-transcription polymerase chain reaction and Western blotting assays. Immunohistochemical staining was used to detect SLC17A9 protein expression in 144 CRC patients in our center. The bioinformatic analysis, Western blotting, and immunohistochemical analyses revealed that SLC17A9 was significantly up-regulated in CRC specimens compared with adjacent nontumorous tissues. SLC17A9 overexpression was significantly correlated with several clinicopathological features, such as advanced T stage ($P < .001$), N stage ($P < .001$), M stage ($P < .001$), TNM stage ($P < .001$), and tumor location ($P = .01$). A Kaplan-Meier survival curve suggested that higher SLC17A9 expression was statistically correlated with poor overall survival and disease-free survival in patients with CRC. Univariate and multivariate Cox regression analyses demonstrated that SLC17A9 was an independent prognostic predictor for survival of CRC patients. Therefore, our data suggested that SLC17A9 may play an important role in the progression of CRC and may potentially be used as an independent biomarker for prognostic evaluation of CRC.

☆ Competing interests: The authors declare that they have no competing interests.

☆☆ Funding/Support: This study was supported by grants from the National Natural Science Foundation of China (81172339), the Science and Technology Foundation of Guangdong Province (2016A020216008), the Natural Science Foundation of Guangdong Province (2017A030310194, S2013020012724, and 2017A030313513), the Postdoctoral Science Foundation of China (2017 M622878), the Medical Science and Technology Research Foundation of Guangdong Province (A2017058), the Science and Technology Planning Project of Guangdong Province (2016A020213002, 2012B060300011, 201510010146), the Medical Scientific Research Foundation of Guangdong Province (A2018022), and the "3 & 3" Project of The First Affiliated Hospital of Sun Yat-sen University (Yulong He).

* Correspondence to: X. Song, Department of Gastrointestinal Surgery, First Affiliated Hospital, Sun Yat-sen University, 58 Zhongshan 2nd Rd, Guangzhou 510080, China.

** Correspondence to: J. Liu, Department of Respiratory Medicine, Guangdong Second People's Hospital, 466 Xingang Middle Rd, Haizhu District, Guangzhou 510317, China.

E-mail addresses: songxm@mail.sysu.edu.cn (X. Song), liujiaSEY@163.com (J. Liu).

[1] Contributed equally to this study.

https://doi.org/10.1016/j.humpath.2018.09.002

1. Introduction

Colorectal cancer (CRC), one of the most common malignant tumors worldwide, is the fourth leading cause of cancer-related death worldwide [1,2]. Many factors are related to the occurrence of CRC, such as lifestyle, genetic mutations, and familial inheritance. However, the mechanism responsible for development of CRC is not clear. A number of genes, including *DPYD*, *KRAS*, *BRAF*, and *UGT1A1*, have been found to be related to the carcinogenesis and progression of CRC [3-5], but the molecular mechanisms remain unknown. Thus, understanding the molecular mechanisms of CRC development and progression may help us to find new therapeutic strategies.

Solute carrier family 17 member 9 (*SLC17A9*), also known as vesicular nucleotide transporter, belongs to the family of SLC-17 [6]. This gene encodes a member of a family of transmembrane proteins that are involved in the transport of small molecules [7]. The encoded protein participates in the vesicular uptake, storage, and secretion of adenosine triphosphate (ATP) and other nucleotides [8-11]. Recent studies have indicated that SLC17A9 activity mediates lysosomal ATP accumulation and plays an important role in lysosomal physiology and cell viability [12]. Moreover, studies have confirmed that SLC17A9 may promote chromosome 20q amplicon-driven colorectal adenoma to carcinoma progression [13]. Collectively, these studies suggest that SLC17A9 is critical to cell ATP transport and cell viability. However, whether SLC17A9 could serve as an oncogene and regulate the progression and development of CRC remains poorly understood. Therefore, the present study was conducted to detect the expression of SLC17A9 in CRC and analyze the relationship between the clinical significance in CRC and the expression of SLC17A9.

2. Materials and methods

2.1. Tissues specimens

Patient consent and ethical approval from the First Affiliated Hospital of Sun Yat-Sen University (FAHSYSU) institutional review board were obtained for the use of these clinical materials for research purposes.

Eight fresh, paired CRC and adjacent nontumorous tissues from surgical resection specimens were obtained from the FAHSYSU. None of the patients received chemotherapy or radiotherapy or other treatments before sampling. These samples were snap-frozen in liquid nitrogen and then stored at −80°C.

One hundred forty-four cases of CRC paraffin-embedded tissues were obtained from the Department of Pathology FAHSYSU. All patients included in this study have received surgical treatment at FAHSYSU in 2011, and follow-ups were terminated by December 2017.

2.2. Quantitative real-time reverse-transcription polymerase chain reaction

Total RNA was isolated using RNA plus reagent (TaKaRa, Tokyo, Japan). Complementary DNA was prepared using oligodT primers according to the protocol supplied with the Primer Script TM RT Reagent (TaKaRa). Expression of *SLC17A9* was determined by quantitative real-time reverse-transcription polymerase chain reaction (qRT-PCR) using Power SYBR green PCR master mix (Applied Biosystems Carlsbad, California, USA). primer sequences were as follows: *SLC17A9*, (forward: 5′-AGGGGTTTACTTCCCTGCC-3′, reverse: 5′-GTCAGCAGCGTCCCAAACT-3′); *GAPDH*, (forward: 5′-CGCTGAGTACGTCGTGGAGTC-3′ and reverse: 5′-GCTGATGATCTTGAGGCTGTTGTC-3′).

2.3. Immunohistochemical staining

For immunohistochemistry (IHC), deparaffinized tissue sections were pretreated with 10 mM sodium citrate buffer (pH 6.0, boiling temperature, high pressure, 10 minutes), cooled for 1 hour at room temperature, immersed in 3% hydrogen peroxide (H_2O_2) for 10 minutes to block endogenous peroxidase, blocked with 5% goat serum diluted in phosphate-buffered saline at room temperature for 30 minutes, incubated at 4°C overnight in a humidified chamber with primary antibody against SLC17A9 antibody (1:400; Millipore, Billerica, MA), rinsed, and incubated with horseradish peroxidase–conjugated secondary antibody using an Envision Detection Kit, GK500705 (Gene Tech, Shanghai, China). Targeted protein was visualized using 3,3′-diaminobenzidine as the substrate.

IHC evaluation was performed by 2 investigators who were blinded to the sample. The resulting slides were assessed and scored according to the percentage of positive tumor cells as follows: the percentage of positive staining was defined as 0 (none positive staining cells), 1 (<20% of positive staining cells), 2 (20%-50% of positive staining cells) or 3 (>50% of positive staining cells). The staining intensity was scored as follows: 0 (negative), 1 (weak), 2 (moderated), and 3 (strong). Each section was assigned a final expression score by adding the intensities of the immunoreactivities and the proportion of stained tumor cells, which resulted in scores of 0 or 2 to 7. To analyze the prognostic value of SLC17A9 expression, we stipulated that scores of 0 to 3 were counted as low expression, whereas scores of 4 to 7 were counted as overexpression [14].

2.4. Western blotting analysis

Freshly frozen tissue specimens were homogenized in cell lysis buffer (KeyGene, Nanjing, China), and the protein concentration was quantified with an Enhanced BCA Protein Assay Kit (KeyGene, Nanjing, China). Protein was separated by 8% to 10% sodium dodecyl sulfate polyacrylamide gel electrophoresis and electrotransferred to polyvinylidene gel electrophoresis membranes (Millipore). The membranes were

immersed in Tris-buffered saline (TBS) containing 0.1% Tween 20 and 5% bovine serum albumin for 2 hours at room temperature to block the nonspecific binding. Subsequently, the membranes were incubated overnight at 4°C with anti-SLC17A9 antibody (1:1000; Millipore, lot: 2952320), anti-GAPDH (1:1000; Proteintech, Wuhan, China, 430223, lot: AG02237527) primary antibodies. Then, the membranes were washed with TBS–0.1% Tween 20 and incubated with horseradish peroxidase–conjugated goat antirabbit antibody (1:5000; Cell Signaling Technology, Danvers, MA,USA) at room temperature for 1 hour. The membranes were washed with TBS–0.1% Tween 20 three times and visualized using enhanced chemiluminescence detection reagent with an enhanced chemiluminescence kit (Millipore).

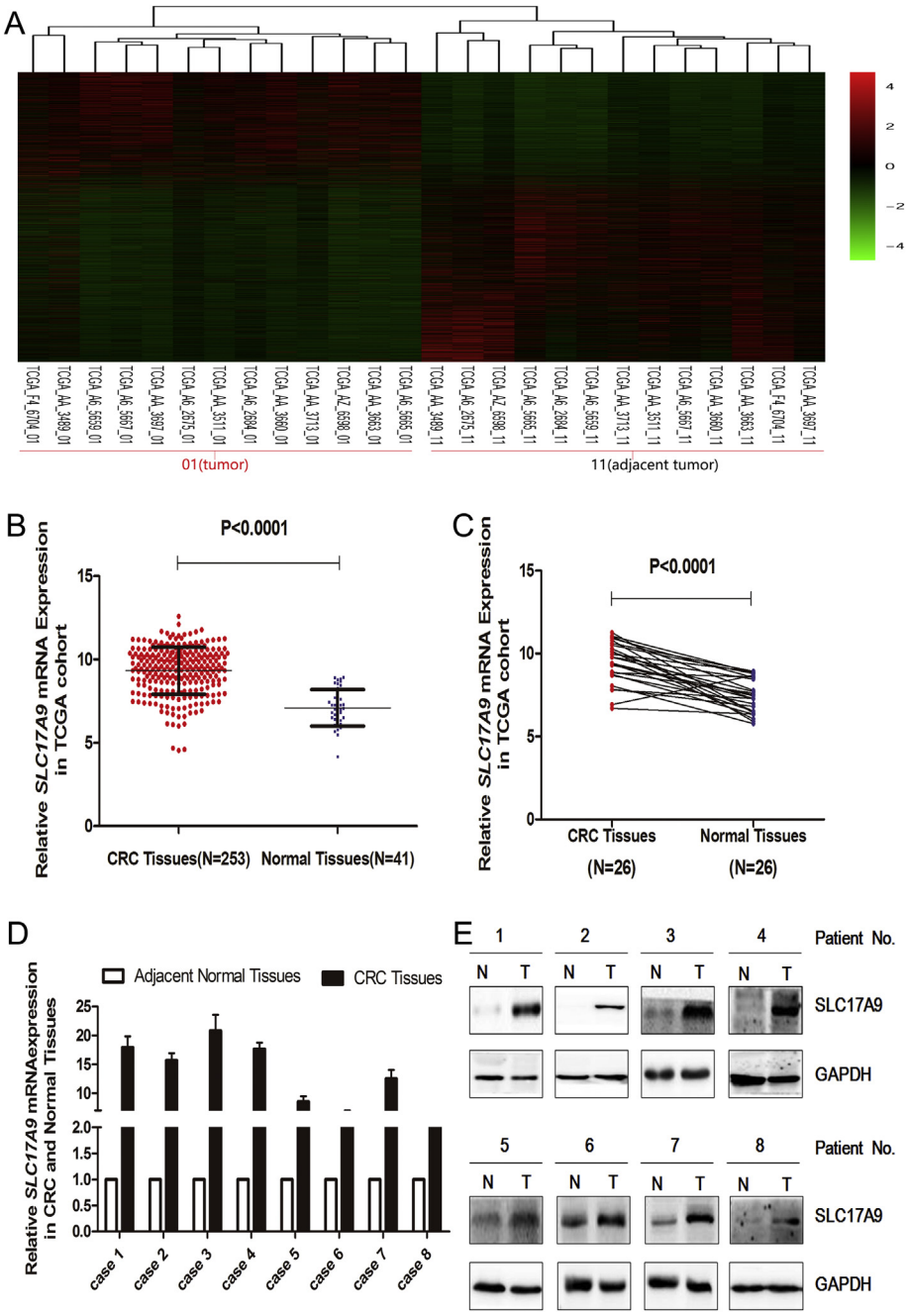

Fig. 1 Up-regulation of SLC17A9 in CRC. A, Analysis of 13 pairs of TCGA chip data in the heat map. B, analysis of *SLC17A9* expression in unpaired CRC (n = 253) and normal tissues (41) in the TCGA cohort ($P < .001$). C, *SLC17A9* expression in paired normal and CRC tissues (n = 32) in the TCGA cohort ($P < .001$). D, The mRNA expression of SLC17A9 is up-regulated in 10 paired CRC tissues compared with matched adjacent nontumor tissues, analyzed by qRT-PCR analysis. E, Representative results of expression levels of *SLC17A9* protein in 10 CRC tissues and matched adjacent nontumor tissues. T, CRC tissues; N, matched nontumor tissues.

Table 1 Oncomine analysis of *SLC17A9* expression in CRC (total of 8 CRC cohorts)

Cohort	Sample (n)	*t* Test	Fold change	*P*
Skrzypczak et al [15], Colorectal 2	Colon carcinoma (5) *vs* normal (10)	13.68	3.544	1.42×10^{-8}
	Colon carcinoma epithelia (5) *vs* normal (10)	8.278	2.833	1.19×10^{-6}
	Colon adenoma (5) *vs* normal (10)	3.912	1.419	.001
	Colon adenoma epithelia (5) *vs* normal (10)	2.411	1.31	.016
Kaiser et al [16], Colon	Rectal mucinous adenocarcinoma (4) *vs* normal (5)	3.214	1.65	.014
	Cecum adenocarcinoma (17) *vs* normal (5)	3.667	1.418	.002
	Rectosigmoid adenocarcinoma (10) *vs* normal (5)	6.009	2.04	2.24×10^{-5}
	Colon adenocarcinoma (41) *vs* normal (5)	7.811	1.853	6.78×10^{-5}
	Colon mucinous adenocarcinoma (13) *vs* normal (5)	6.093	1.829	2.46×10^{-5}
	Rectal adenocarcinoma (8) *vs* normal (5)	5.585	1.85	8.33×10^{-5}
Hong et al [17], Colorectal	Colorectal carcinoma (70) *vs* normal (12)	7.866	3.054	2.81×10^{-9}
	Cecum adenocarcinoma (22) *vs* NORMAL (22)	6.391	1.771	5.59×10^{-8}
	Colon mucinous adenocarcinoma (22) *vs* normal (22)	6.445	1.997	5.87×10^{-8}
TCGA Colorectal	Rectosigmoid adenocarcinoma (3) *vs* normal (22)	4.294	2.093	.014
	Colon adenocarcinoma (101) *vs* normal (22)	9.569	2.216	4.06×10^{-13}
	Rectal adenocarcinoma (60) *vs* normal (22)	9.93	2.264	2.48×10^{-13}
	Rectal mucinous adenocarcinoma (6) *vs* normal (22)	6.049	2.362	1.56×10^{-4}
Notterman et al [18], Colon	Colon adenocarcinoma (18) *vs* normal (18)	1.912	1.42	.032
Skrzypczak et al [15], Colorectal	Colorectal carcinoma (36) *vs* normal (24)	3.879	1.277	1.36×10^{-4}
	Colorectal adenocarcinoma (45) *vs* normal (24)	3.255	1.181	.001
Sabates-Bellver et al [19], Colon	Rectal adenoma (7) *vs* normal (32)	3.138	1.619	.003
	Colon adenoma (25) *vs* normal (32)	3.925	1.687	1.22×10^{-4}
Gaedcke et al [20], Colorectal	Rectal adenocarcinoma (65) *vs* normal (65)	1.803	1.154	.037

2.5. Bioinformatics analysis

The RNASeq data for CRC were downloaded from The Cancer Genome Atlas (TCGA) databases (https://genome-cancer.ucsc.edu). The data were log2 transformed and analyzed using Excel 2001 and GraphPad Prism 5.0 software.

2.6. Statistical analysis

SPSS version 18.0 (IBM, Armonk, NY) was used for analyzing the data. The relationship between SLC17A9 expression and features of tumor progression was analyzed using the χ^2 tests. Kaplan-Meier survival curves were constructed, and the log-rank test was carried out using univariate analysis. Multivariate analysis was performed using Cox proportional hazards model. Differences were considered to be statistically significant at *P* values of .05 for all analyses.

3. Results

3.1. Overexpression of SLC17A9 in CRC tissues

We analyzed 13 pairs of CRC chip data from TCGA-CRC data set and found that many genes are up- or down-regulated in CRC samples compared with normal samples and SLC17A9 was significantly overexpressed in CRC tissues (01) compared with adjacent normal tissues (11; Fig. 1A). To confirm the expression of *SLC17A9* in CRC and normal tissues, we analyzed *SLC17A9* expression in all cases of CRC and normal sample from TCGA cohort (Fig. 1B and C). The messenger RNA (mRNA) level of *SLC17A9* in the unpaired CRC (n = 263) and normal tissues (n = 41) from the TCGA cohorts indicated that *SLC17A9* mRNA expression was remarkably up-regulated in CRC tissues ($P < .001$; Fig. 1B). Similarly, the up-regulation of *SLC17A9* mRNA in CRC was confirmed in paired tumor and adjacent nontumor tissues in TCGA cohorts (n = 26, $P < .001$; Fig. 1C). We can see an analogous result in other CRC cohorts from the Oncomine database (Table 1) [15,21-25]. To verify the overexpression status of SLC17A9 in CRC tissues, the qRT-PCR and Western blotting assays were used to detect *SLC17A9* expression level in 8 fresh paired specimens in CRC patients from our medical center, and we found that *SLC17A9* mRNA (Fig. 1D) and protein (Fig. 1E) levels were elevated in CRC tissues compared with adjacent nontumor tissues. Taken together, we confirmed that SLC17A9 was up-regulated in CRC tissues.

3.2. Correlation between SLC17A9 expression and clinicopathological parameters in patients with CRC

To estimate the relationship between SLC17A9 expression and clinicopathological variables in human CRCs, 144 paraffin-embedded primary CRC samples were used to examine SLC17A9 expression using IHC staining. As shown in Fig. 2, SLC17A9-positive staining mainly distributed in cancer cell cytoplasm and cytomembrane (Fig. 2A-D).

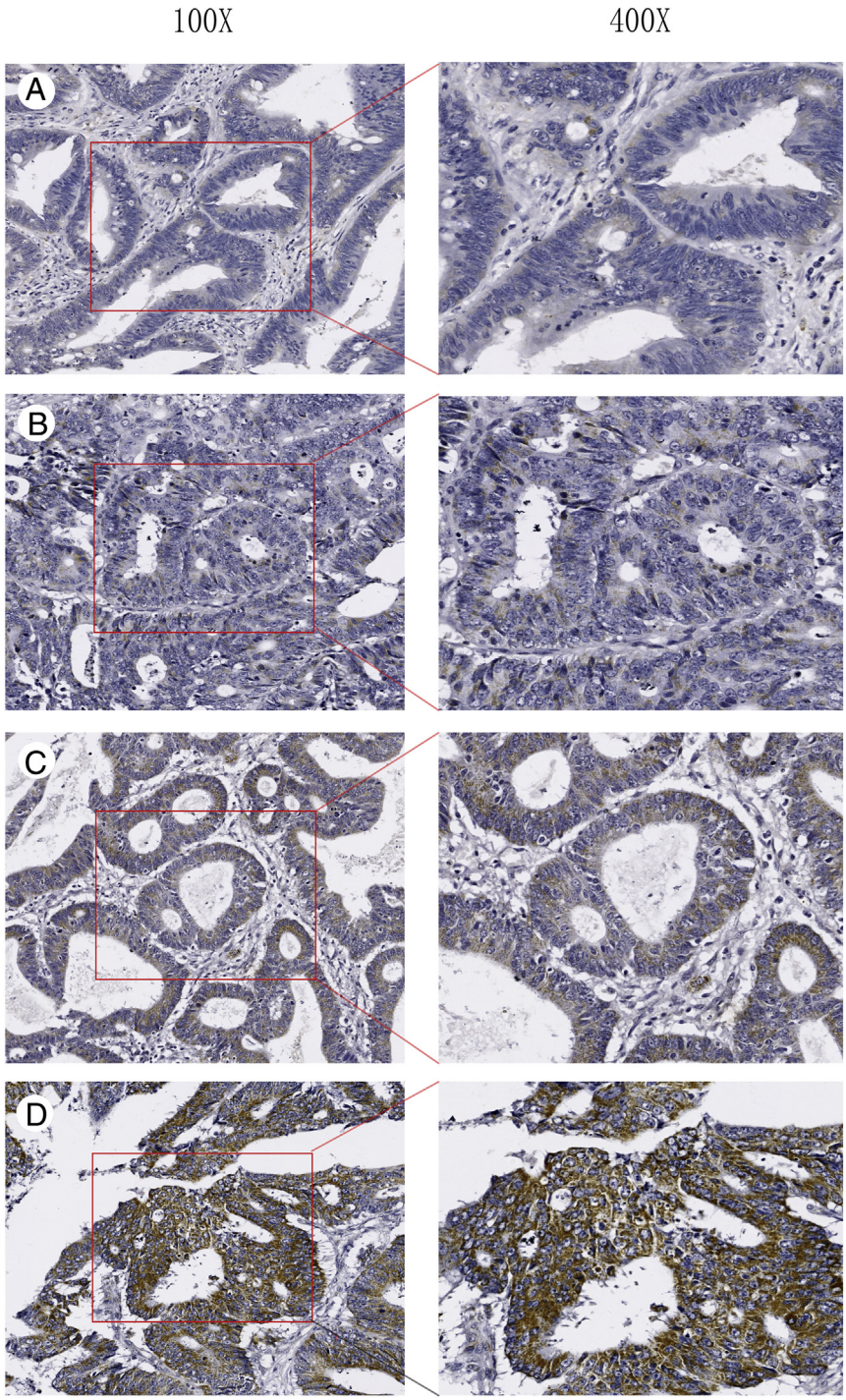

Fig. 2 IHC analysis of SLC17A9 protein expression in CRC tissues. A, Negative expression of SLC17A9 was observed in CRC tissues (case 25), in which no tumor cells demonstrated staining of SLC17A9. B, Low expression of SLC17A9 was observed in a CRC tissue (case 50), in which less than 20% of tumor cells demonstrated staining of SLC17A9. C, Another CRC (case 39) tissue showed high expression of SLC17A9, in which 20% to 50% of tumor cells demonstrated staining of SLC17A9. D, High expression of SLC17A9 was detected in a CRC tissue (case 30).

To evaluate the role of SLC17A9 protein in CRC progression, we analyzed correlations between SLC17A9 protein expression and major clinicopathological features as shown in Table 2.

SLC17A9 overexpression in CRC tissues was significantly related to larger tumor size ($P = .008$), tumor location ($P = .004$), advanced Duke stage ($P < .001$), T stage ($P < .001$), N stage ($P < .001$), M stage ($P = .031$), and TNM stage ($P < .001$). However, SLC17A9 expression was not found to be significantly related to other clinicopathological features, such as sex ($P = .605$), age ($P = .735$), and differentiation degree ($P = .604$).

Table 2 Correlations between STIP1 expression and clinicopathological variables of 144 CRC patients

Characteristics	No.	Low SLC17A9 expression (n = 81)	High SLC17A9 expression (n = 63)	χ^2	*P*
Sex					
Male	88	51	37	0.267	.605
Female	56	30	26		
Age (y)					
<60	64	35	29	0.114	.735
≥60	80	46	34		
Tumor size (cm)					
<5	71	43	28	1.059	.303
≥5	73	38	35		
Differentiation degree					
Well	7	5	2		
Moderate	107	58	49	1.008	.604
Poor	30	18	12		
Tumor location					
Ascending colon	31	13	18		
Transverse colon	9	7	2		
Descending colon	7	1	6	13.38	.01
Sigmoid colon	27	13	14		
Rectum	70	47	23		
TNM stage					
I	20	20	0		
IIa	32	31	1		
IIb	8	4	4		
IIc	19	2	17		
IIIa	18	18	0	105.78	<.001
IIIb	14	4	10		
IIIc	14	0	14		
IV	19	2	17		

3.3. Relationship between patient survival, SLC17A9 protein expression, and clinicopathological parameters

The follow-up period of the 144 CRC patients ranged from 4 to 91 months, with a mean survival time of 66.7 ± 2.7 months. The 5-year overall survival (OS) rate was 59.7%. From the statistical data, we found that patients with SLC17A9 high expression had poor OS ($P < .001$). The 5-year OS rate was 71.6% and 50.8% in the low and high SLC17A9 expression groups, respectively. Furthermore, high SLC17A9 expression indicated a worse disease-free survival (DFS) in patients with CRC ($P < .001$). Moreover, we also detected the prognosis of SLC17A9 expression in early (TNM stages I and II) and advanced (TNM stages III and IV) CRC. The results showed that in early-stage CRC, patients with high SLC17A9 expression in CRC tissues had worse OS than did patients with low SLC17A9 expression in CRC tissues (Fig. 3B, left panel; $P < .001$); however, DFS is not correlated with SLC17A9 overexpression status in early-stage CRC (Fig. 3B, left panel; $P = .203$). Our data also show that patients with high SLC17A9 expression had a worse OS (Fig. 3C, left panel; $P < .001$) and DFS (Fig. 3C, right panel; $P < .001$) than did those with low SLC17A9 expression in advanced CRC.

To identify whether SLC17A9 expression could predict the outcome of patients with CRC, univariate and multivariate analyses were performed to compare the impact of SLC17A9 expression and other clinicopathological factors on the prognosis of CRC patients. Univariate analysis showed that clinical variables, including tumor size, differentiation degree, T stage, N stage, M stage, TNM stage, and SLC17A9 expression, were significantly associated with OS. Furthermore, multivariate Cox regression analysis indicated that SLC17A9 expression ($P = .008$) was an independent predictor of OS in CRC patients (Table 3). In addition, SLC17A9 overexpression ($P = .016$) was associated with DFS in CRC patients (Table 4). Our results indicated that higher SLC17A9 expression level is associated with poor prognosis in CRC patients, suggesting that SLC17A9 might serve as a molecular prognostic marker for CRC.

4. Discussion

In this study, we showed that SLC17A9 is overexpressed at both the mRNA and protein levels in CRC tissues using Western blotting, IHC, and qRT-PCR assays. We firstly identified that SLC17A9 could be a potential new biomarker to evaluate the prognosis of patients with CRC. Also, we demonstrated the correlation between the expression of SLC17A9 and the clinicopathological characteristics in CRC through bioinformatics analysis and the data from the TCGA cohort and Oncomine database [26,27]. First, we detected the *SLC17A9* mRNA level from the data, and the result indicated that SLC17A9 expression was significantly higher in CRC tissues than that in nontumorous tissues. Then, we tested the expression of *SLC17A9* mRNA and protein in fresh CRC tissues and adjacent noncancer tissues. The results were the same as the bioinformatics analysis. Furthermore, we performed IHC staining and analysis in 144 cases of CRC and found that the expression of SLC17A9 protein was significantly higher than that in adjacent normal colorectal tissues. High SLC17A9 expression predicted patients with advanced malignant tumor progression and poor OS and recurrence-free survival. SLC17A9 protein expression was an independent prognostic factor for OS and recurrence-free survival.

In a previous study, we found that SLC17A9 is a functional gene located at human chromosome 20q13.33, in which mutation was found in individuals with autosomal dominant disseminated superficial actinic porokeratosis-8 [28-31]. Emerging evidence has shown that SLC17A9, the vesicular nucleotide transporter, functions in ATP transport across secretory vesicle/granule membranes in astrocytes cells, T cells, and pancreatic cells [9,32,33]. Few studies to date have reported the significance of SLC17A9 in cancer. However,

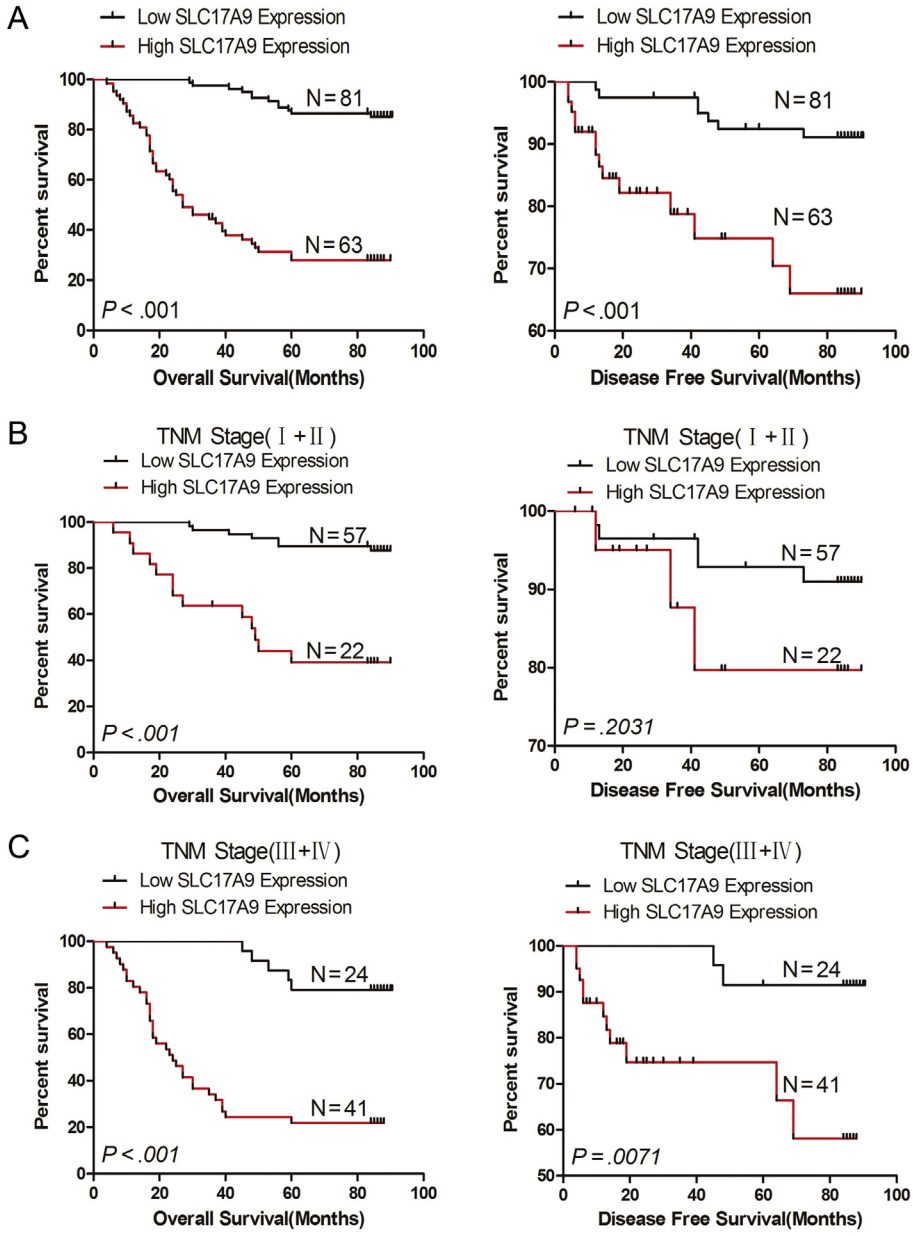

Fig. 3 Kaplan-Meier analysis of association of SLC17A9 expression with patient survival. A, Patients with high SLC17A9 expression had worse DFS (right panel) and OS (left panel) compared with low SLC17A9 expression ($P < .001$). B, Prognostic value of SLC17A9 expression in early stage CRC patients (TNM stages I and II). C, In the late stage, DFS rate of patients (right panel; $P = .0071$) and OS of patients (left panel; $P < .001$) with high SLC17A9 expression was lower than that of those with low SLC17A9 expression (TNM stages III and IV).

Takai et al [34] have reported that SLC17A9 knockdown can inhibit the exocytosis of ATP and decrease cell migration in human lung cancer cells. Similarly, a previous study showed that SLC17a9 protein also functions as a lysosomal ATP transporter and regulates cell viability [12].

However, few studies to date have reported an association between SLC17A9 expression and CRCs. To our knowledge, this is the first demonstration that SLC17A9 is overexpressed in CRC tissues, and SLC17A9 is a prognostic factor for OS in CRC patients. Our finding therefore improves our understanding of the roles of SLC17A9 in the progression of CRC. A limitation of our study is that the impact of SLC17A9 on CRC and its mechanisms have not been reported. SLC17A9 protein is known to be highly enriched in lysosomes and functions as an ATP transporter in those organelles, and SLC17A9 deficiency has been found to reduce lysosome ATP accumulation and compromise lysosome function [12]. ATP has been found to activate proteases, such as cathepsin D, and increases proteolysis within lysosomes [21] and cathepsin D deficiency–induced lysosomal storage of lipofuscin [22]. Therefore, SLC17A9 function suppression

Table 3 Cox propotional harzard regression analysis for OS

Characteristics	Univariate analysis				Multivariate analysis			
	Harzard ratio	*P*	95% Confidence interval		Harzard ratio	*P*	95% Confidence linterval	
			Lower	Upper			Lower	Upper
Sex	1.406	.201	0.834	2.367				
Age	0.988	.209	0.97	1.007				
Tumor size	1.868	.022	1.095	3.186	1.387	.255	0.789	2.437
Differentiation degree	3.264	<.001	1.944	5.481	3.004	<.001	1.741	5.183
Tumor location	1.066	.452	0.903	1.257				
T stage	2.634	.002	1.424	4.872				
N stage	1.706	.001	1.235	2.357				
M stage	4.295	<.001	2.355	7.833				
TNM stage	2.233	<.001	1.631	3.059				
SLC17A9 expression	2.008	.009	1.186	3.4	2.033	.008	1.199	3.446

could attenuate cathepsin D activity and promote subsequent lipofuscin accumulation and cell death. Others have reported that lysosomal ATP release via lysosomal exocytosis is implicated in cell migration [23]. Tumor buds are defined as single cells or small clusters of de-differentiated tumor cells at the invasive front, which is highly relevant to epithelial-mesenchymal transition in tumor progression [24,25]. We hypothesized that overexpression of SLC17A9 may promote the formation of tumor buds through the epithelial-mesenchymal transition pathway and then lead to poor prognosis in CRC. Therefore, our future studies will explore the molecular mechanisms of SLC17A9 functions on CRC.

In conclusion, our results showed that the *SLC17A9* gene is frequently amplified in CRC, which is associated with significant mRNA and protein overexpression. High SLC17A9 expression played an important role in CRC development and progression. Our finding indicated that SLC17A9 may serve as a new prognostic and potential therapeutic target in CRC.

Author contributions

X. S. and J. L. designed the research; L. Y., Z. C., W. X., H. R., E. Z., K. X., H. Y., Z. Z., L. D., and Y. H. performed the research; L. Y. and Z. C. analyzed the data; and L. Y. wrote the manuscript.

Availability of data and materials

The data sets used and analyzed during the current study are available from the corresponding authors on reasonable request.

Ethics approval and consent to participate

All procedures performed in studies were in accordance with the ethical standards of the Ethics Committee of the

Table 4 Cox propotional harzard regression analysis for DFS

Characteristics	Univariate analysis				Multivariate analysis			
	Harzard ratio	*P*	95% Confidence interval		Harzard ratio	*P*	95% Confidence interval	
			Lower	Upper			Lower	Upper
Sex	1.02	.965	0.423	2.461				
Age	0.991	.573	0.961	1.022				
Tumor size	0.837	.688	0.352	1.99				
Differentiation degree	0.987	.979	0.381	2.559				
Tumor location	1.091	.539	0.827	1.439				
T stage	1.811	.221	0.7	4.684				
N stage	1.596	.091	0.928	2.745				
M stage	4.772	.002	1.807	12.601	3.04	.189	0.578	15.989
TNM stage	2.064	.006	1.233	3.454	0.225	.236	0.019	2.66
SLC17A9 expression	3.06	.016	1.232	7.601	2.018	.23	0.642	6.347

Institutional Ethical Review Board of the First Affiliated Hospital, Sun Yat-sen University.

References

[1] Torre LA, Bray F, Siegel RL, Ferlay J, Lortet-Tieulent J, Jemal A. Global cancer statistics, 2012. CA Cancer J Clin 2015;65:87-108. https://doi.org/10.3322/caac.21262.

[2] Chen W, Zheng R, Baade PD, et al. Cancer statistics in China, 2015. CA Cancer J Clin 2016;66:115-32. https://doi.org/10.3322/caac.21338.

[3] De Roock W, Claes B, Bernasconi D, et al. Effects of *KRAS*, *BRAF*, NRAS, and PIK3CA mutations on the efficacy of cetuximab plus chemotherapy in chemotherapy-refractory metastatic colorectal cancer: a retrospective consortium analysis. Lancet Oncol 2010;11:753-62. https://doi.org/10.1016/S1470-2045(10)70130-3.

[4] Cremolini C, Del Re M, Antoniotti C, et al. *DPYD* and *UGT1A1* genotyping to predict adverse events during first-line FOLFIRI or FOLFOXIRI plus bevacizumab in metastatic colorectal cancer. Oncotarget 2018;9:7859-66. https://doi.org/10.18632/oncotarget.23559.

[5] Obuch JC, Ahnen DJ. Colorectal cancer: genetics is changing everything. Gastroenterol Clin North Am 2016;45:459-76. https://doi.org/10.1016/j.gtc.2016.04.005.

[6] Sreedharan S, Shaik JH, Olszewski PK, Levine AS, Schioth HB, Fredriksson R. Glutamate, aspartate and nucleotide transporters in the SLC17 family form four main phylogenetic clusters: evolution and tissue expression. BMC Genomics 2010;11:17. https://doi.org/10.1186/1471-2164-11-17.

[7] Bissa B, Beedle AM, Govindarajan R. Lysosomal solute carrier transporters gain momentum in research. Clin Pharmacol Ther 2016;100:431-6. https://doi.org/10.1002/cpt.450.

[8] Sawada K, Echigo N, Juge N, et al. Identification of a vesicular nucleotide transporter. Proc Natl Acad Sci U S A 2008;105:5683-6. https://doi.org/10.1073/pnas.0800141105.

[9] Oya M, Kitaguchi T, Yanagihara Y, et al. Vesicular nucleotide transporter is involved in ATP storage of secretory lysosomes in astrocytes. Biochem Biophys Res Commun 2013;438:145-51. https://doi.org/10.1016/j.bbrc.2013.07.043.

[10] Sesma JI, Kreda SM, Okada SF, et al. Vesicular nucleotide transporter regulates the nucleotide content in airway epithelial mucin granules. Am J Physiol Cell Physiol 2013;304:C976-84. https://doi.org/10.1152/ajpcell.00371.2012.

[11] Zhong XZ, Cao Q, Sun X, Dong XP. Activation of lysosomal P2X4 by ATP transported into lysosomes via VNUT/SLC17A9 using V-ATPase generated voltage gradient as the driving force. J Physiol 2016;594:4253-66. https://doi.org/10.1113/JP271893.

[12] Cao Q, Zhao K, Zhong XZ, et al. SLC17A9 protein functions as a lysosomal ATP transporter and regulates cell viability. J Biol Chem 2014;289:23189-99. https://doi.org/10.1074/jbc.M114.567107.

[13] Sillars-Hardebol AH, Carvalho B, Tijssen M, et al. TPX2 and AURKA promote 20q amplicon-driven colorectal adenoma to carcinoma progression. Gut 2012;61:1568-75. https://doi.org/10.1136/gutjnl-2011-301153.

[14] Wang D, Zhang S, Chen Y, Hu B, Lu C. Low expression of NKD2 is associated with enhanced cell proliferation and poor prognosis in human hepatocellular carcinoma. Hum Pathol 2018;72:80-90. https://doi.org/10.1016/j.humpath.2017.09.016.

[15] Skrzypczak M, Goryca K, Rubel T, et al. Modeling oncogenic signaling in colon tumors by multidirectional analyses of microarray data directed for maximization of analytical reliability. PLoS One 2010;5. https://doi.org/10.1371/journal.pone.0013091 [5:e13091].

[16] Kaiser S, Park YK, Franklin JL, et al. Transcriptional recapitulation and subversion of embryonic colon development by mouse colon tumor models and human colon cancer. Genome Biol 2007;8:R131. https://doi.org/10.1186/gb-2007-8-7-r131.

[17] Hong Y, Downey T, Eu KW, Koh PK, Cheah PY. A 'metastasis-prone' signature for early-stage mismatch-repair proficient sporadic colorectal cancer patients and its implications for possible therapeutics. Clin Exp Metastasis 2010;27:83-90. https://doi.org/10.1007/s10585-010-9305-4.

[18] Notterman DA, Alon U, Sierk AJ, Levine AJ. Transcriptional gene expression profiles of colorectal adenoma, adenocarcinoma, and normal tissue examined by oligonucleotide arrays. Cancer Res 2001;61:3124-30.

[19] Sabates-Bellver J, Van der Flier LG, de Palo M, et al. Transcriptome profile of human colorectal adenomas. Mol Cancer Res 2007;5:1263-75. https://doi.org/10.1158/1541-7786.MCR-07-0267 [MCR].

[20] Gaedcke J, Grade M, Jung K, et al. Mutated *KRAS* results in overexpression of DUSP4, a MAP-kinase phosphatase, and SMYD3, a histone methyltransferase, in rectal carcinomas. Genes Chromosomes Cancer 2010;49:1024-34. https://doi.org/10.1002/gcc.20811.

[21] Pillai S, Zull JE. Effects of ATP, vanadate, and molybdate on cathepsin D–catalyzed proteolysis. J Biol Chem 1985;260:8384-9.

[22] Koike M, Nakanishi H, Saftig P, et al. Cathepsin D deficiency induces lysosomal storage with ceroid lipofuscin in mouse CNS neurons. J Neurosci 2000;20:6898-906.

[23] Dou Y, Wu HJ, Li HQ, et al. Microglial migration mediated by ATP-induced ATP release from lysosomes. Cell Res 2012;22:1022-33. https://doi.org/10.1038/cr.2012.10.

[24] Hong KO, Oh KY, Shin WJ, Yoon HJ, Lee JI, Hong SD. Tumor budding is associated with poor prognosis of oral squamous cell carcinoma and histologically represents an epithelial-mesenchymal transition process. Hum Pathol 2018. https://doi.org/10.1016/j.humpath.2018.06.012.

[25] De Smedt L, Palmans S, Andel D, et al. Expression profiling of budding cells in colorectal cancer reveals an EMT-like phenotype and molecular subtype switching. Br J Cancer 2017;116:58-65. https://doi.org/10.1038/bjc.2016.382.

[26] Zhu Y, Qiu P, Ji Y. TCGA-Assembler: open-source software for retrieving and processing TCGA data. Nat Methods 2014;11:599. https://doi.org/10.1038/nmeth.2956.

[27] Rhodes DR, Yu J, Shanker K, et al. ONCOMINE: a cancer microarray database and integrated data-mining platform. Neoplasia 2004;6:1-6.

[28] Cui H, Li L, Wang W, et al. Exome sequencing identifies SLC17A9 pathogenic gene in two Chinese pedigrees with disseminated superficial actinic porokeratosis. J Med Genet 2014;51:699-704. https://doi.org/10.1136/jmedgenet-2014-102486.

[29] Dereure O. Mutation in the SLC17A9 gene in familial superficial actinic disseminated porokeratosis. Ann Dermatol Venereol 2015;142:155-6. https://doi.org/10.1016/j.annder.2014.12.004.

[30] Li M, Li Z, Wang J, et al. Mutations in the mevalonate pathway genes in Chinese patients with porokeratosis. J Eur Acad Dermatol Venereol 2016;30:1512-7. https://doi.org/10.1111/jdv.13653.

[31] Li X, Zhou Q, Zhu L, et al. Analysis of clinical and genetic features of nine patients with disseminated superfacial actinic porokeratosis. Zhonghua Yi Xue Yi Chuan Xue Za Zhi 2017;34:481-5. https://doi.org/10.3760/cma.j.issn.1003-9406.2017.04.003.

[32] Haanes KA, Kowal JM, Arpino G, et al. Role of vesicular nucleotide transporter VNUT (SLC17A9) in release of ATP from AR42J cells and mouse pancreatic acinar cells. Purinergic Signal 2014;10:431-40. https://doi.org/10.1007/s11302-014-9406-7.

[33] Chen B, Jiang L, Zhong ML, et al. Identification of fusion genes and characterization of transcriptome features in T-cell acute lymphoblastic leukemia. Proc Natl Acad Sci U S A 2018;115:373-8. https://doi.org/10.1073/pnas.1717125115.

[34] Takai E, Tsukimoto M, Harada H, Sawada K, Moriyama Y, Kojima S. Autocrine regulation of TGF-beta1–induced cell migration by exocytosis of ATP and activation of P2 receptors in human lung cancer cells. J Cell Sci 2012;125:5051-60. https://doi.org/10.1242/jcs.104976.